Development 134, 3495-3505 (2007) doi:10.1242/dev.000802

Functions of the novel RhoGAP proteins RGA-3 and RGA-4 in the germ line and in the early embryo of *C. elegans*

Cornelia Schmutz, Julia Stevens and Anne Spang*

We have identified two redundant GTPase activating proteins (GAPs) – RGA-3 and RGA-4 – that regulate Rho GTPase function at the plasma membrane in early *Caenorhabditis elegans* embryos. Knockdown of both RhoGAPs resulted in extensive membrane ruffling, furrowing and pronounced pseudo-cleavages. In addition, the non-muscle myosin NMY-2 and RHO-1 accumulated on the cortex at sites of ruffling. RGA-3 and RGA-4 are GAPs for RHO-1, but most probably not for CDC-42, because only RHO-1 was epistatic to the two GAPs, and the GAPs had no obvious influence on CDC-42 function. Furthermore, knockdown of either the RHO-1 effector, LET-502, or the exchange factor for RHO-1, ECT-2, alleviated the membrane-ruffling phenotype caused by simultaneous knockdown of both RGA-3 and RGA-4 [*rga-3/4 (RNAi)*]. GFP::PAR-6 and GFP::PAR-2 were localized at the anterior and posterior part of the early *C. elegans* embryo, respectively showing that *rga-3/4 (RNAi)* did not interfere with polarity establishment. Most importantly, upon simultaneous knockdown of RGA-3, RGA-4 and the third RhoGAP present in the early embryo, CYK-4, NMY-2 spread over the entire cortex and GFP::PAR-2 localization at the posterior cortex was greatly diminished. These results indicate that the functions of CYK-4 are temporally and spatially distinct from RGA-3 and RGA-4 (RGA-3/4). RGA-3/4 and CYK-4 also play different roles in controlling LET-502 activation in the germ line, because *rga-3/4 (RNAi)*, but not *cyk-4 (RNAi)*, aggravated the *let-502(sb106)* phenotype. We propose that RGA-3/4 and CYK-4 control with which effector molecules RHO-1 interacts at particular sites at the cortex in the zygote and in the germ line.

KEY WORDS: RhoGAP, *C. elegans*, Acto-myosin, Early embryo, Germ line

INTRODUCTION

Asymmetric cell division is a general mechanism by which to generate two non-identical daughter cells. One of the most-studied systems is the first asymmetric division of the *Caenorhabditis elegans* embryo (Cowan and Hyman, 2004a; Gönczy et al., 2001; Schneider and Bowerman, 2003). After fertilization, the egg completes the meiotic divisions and extrudes two polar bodies. During the meiosis events, right after sperm entry, the entire cortex of the embryo is highly contractile. The sperm initiates cortical and cytoplasmic movements, which are actin-dependent. These streamings are essential for the establishment of polarity. How they are controlled, however, has remained largely elusive. Upon movement of the maternal pronucleus towards the paternal pronucleus, the posterior part of the cortex smoothens, which is supposedly controlled by the centrosomes brought along by the sperm (Cheeks et al., 2004; Cowan and Hyman, 2004b; Munro et al., 2004). Posterior smoothening and anterior ruffling of the cortex lead to a membrane invagination, called pseudo-cleavage. The two pronuclei meet in the posterior part of the embryo and migrate to towards the middle of the embryo, where mitosis is initiated. Upon centration, cortical ruffling activity ceases, and resumes during anaphase of the first mitosis. After cytokinesis, the larger anterior AB cell and the smaller P1 cell prepare the next division cycle, which is again asymmetric.

The PAR proteins play a crucial role in the setup and maintenance of polarity right after fertilization (Cuenca et al., 2003). Whereas the PAR-3–PAR-6–aPKC complex determines anterior polarity, PAR-1 and PAR-2 occupy the posterior part. The two domains do not intermix and are mutually exclusive. PAR-5 is a 14-3-3 protein that seems to be essential to maintain the two different domains (Kemphues, 2000).

Contractility in most systems involves the acto-myosin system, which is controlled by GTP-binding proteins of the Rho superfamily (Etienne-Manneville and Hall, 2002; Glotzer, 2005). Rho GTPases are molecular switches that exist in an activated, GTP-bound form and an inactive GDP-bound conformation. The switch between the two conformations is achieved by guanine nucleotide exchange factors (GEFs) and GTPase-activating proteins (GAPs) (Bernards, 2003; Schmidt and Hall, 2002). In their activated state, the GTPases can interact with and signal to downstream effectors, which in turn control a variety of cell processes. For example, effectors of RhoA (RHO-1 in *C. elegans*), such as ROCK1 (LET-502) regulate the acto-myosin system. RhoGAPs are particularly interesting proteins, because they often contain multiple functional motifs in addition to the GAP domain that might regulate localization or GAP activity, or might recruit other signalling proteins (Moon and Zheng, 2003). They outnumber RhoGTPases by 4:1 in humans (and 5:1 in *C. elegans*), so, in principle, the action of a given RhoGTPase could be regulated by at least four different RhoGAPs in different spatial and temporal patterns. Their versatility is exemplified by the ARAP proteins, which contain both a RhoGAP domain and an ArfGAP domain, and can thus serve as converging signalling platforms (Krugmann et al., 2002; Miura et al., 2002).

In oocytes, the acto-myosin network is distributed over the entire cortex. Upon fertilization, due to cortical and cytoplasmic rearrangements, the acto-myosin network becomes restricted to the anterior cortex, giving rise to contractions in the anterior region of the embryo and a smooth posterior part. Local contractility in the posterior region appears to be inhibited by a signal from the centrosome (Cowan and Hyman, 2004b; Munro et al., 2004). Interestingly, a more recent study provides evidence for the RhoGAP CYK-4 being the signal for establishing the posterior PAR-2 domain and causing the retraction of the acto-

Biozentrum, University of Basel, Klingelbergstrasse 70, CH-4056 Basel, Switzerland.

*Author for correspondence (e-mail: anne.spang@unibas.ch)

Accepted 24 July 2007

myosin system to the anterior region of the embryo (Jenkins et al., 2006). How contraction is controlled in the anterior embryo, however, remains elusive.

We investigated the role of two RhoGAP proteins, RGA-3 and RGA-4, in the early *C. elegans* embryo and in the germ line. Knockdown of the two RhoGAPs by RNA interference (RNAi) resulted in hyper-contractility of the anterior cortex in the zygote. Although no major defects were detected in polarity establishment, we observed fluctuations in the size of the PAR-6 domain at the anterior cortex. RGA-3 and RGA-4 (RGA-3/4) have overlapping functions in the early embryo, because concomitant knockdown of both proteins yielded the strongest phenotype. RGA-3/4 are GAPs for RHO-1, because RHO-1, but not CDC-42, was epistatic to RGA-3/4. The only other characterized RhoGAP in the early embryo, CYK-4, has non-redundant functions with RGA-3/4, because the phenotypes of the triple knockdown were additive. Furthermore, *rga-3/4* RNAi treatment [*rga-3/4(RNAi)*] enhanced the gonadal defects in *let-502(sb106)* mutants, whereas *cyk-4(RNAi)* had no effect. RGA-3/4 are required to control the activation of the *C. elegans* ROCK LET-502 in the early embryo. We provide evidence that the specificity of RHO-1 is determined by the differential use of RhoGAPs during early *C. elegans* development.

MATERIALS AND METHODS

General methods and strains

C. elegans was cultured and maintained as described previously (Brenner, 1974) on NGM medium at 20°C unless noted otherwise. The *C. elegans* strains N2 and the alleles *let-502(ok1283)* and *let-502(sb106)* (Piekny et al., 2000) were used for time-lapse studies and for the counting of embryonic lethality rates. Transgenic GFP-expressing lines used in this study are listed below:

The following strains were obtained from the *Caenorhabditis* Genetics Center (CGC): strain AZ212, which expresses a GFP::H2B histone fusion in the germ line (Praitis et al., 2001); KK866, a strain with GFP::PAR-2 (Wallenfang and Seydoux, 2000); JJ1473, a strain expressing NMY-2::GFP (Munro et al., 2004); and WH204, a strain expressing GFP::β-tubulin (Strome et al., 2001). JH1512, a strain bearing GFP::PAR-6 fusion (Cuenca et al., 2003) was a gift from Geraldine Seydoux (John Hopkins University Medical School, Baltimore, USA), and SA115, a strain expressing GFP::RHO-1 (Motegi and Sugimoto, 2006), was a gift from Fumio Motegi (RIKEN, Kobe, Japan).

RNAi experiments

For RNAi-by-feeding experiments, plasmid L4440, containing the desired sequence (see Table 1) was transformed into the *Escherichia coli* strain HT115 (Timmons et al., 2001). NGM plates containing 0.5-2.0 mM IPTG and 25 μg/ml carbenicillin were inoculated with transformed HT115 bacteria. The expression of double-stranded RNA (dsRNA) was induced for 6-9 hours at room temperature on plate. Subsequently, L1, dauer larvae or L3 larvae were transferred to these plates. Animals were cultured at 15, 20 or 23°C and their progeny were analyzed.

For RNAi-by-injection experiments, *C. elegans* genomic or cDNA was used as a template to PCR-amplify the desired sequence (Table 1). PCR products were used as templates for in vitro transcription using T7 polymerase (Promega). dsRNA was produced according to the manufacturer's protocol (Promega), purified by phenol/chloroform extraction and resuspended in 20 μl DEPC-H_2O. dsRNA was injected into the gonad of young adult worms, which were subsequently incubated at 20°C. The progeny of injected animals was analyzed.

For RNAi-by-soaking experiments, L3 larvae were incubated for 24 hours in dsRNA solution in a wet chamber. The animals were transferred onto an agar plate seeded with OP50 bacteria for recovery. The progeny was analyzed.

Live-embryo imaging

Embryos were mounted in a drop of M9 buffer ('hanging drop' method) and covered with a cover slip. Embryos were imaged with a Zeiss Axioplan 2 microscope equipped with a Zeiss Axio Cam MRm camera (Carl Zeiss, Aalen Oberkochen, Germany) and a Plan Apochromat 63×/NA1.40 objective. Zeiss Axiovision 3.1 software was used to control hardware and to acquire and process images. Confocal images were captured with a Leica confocal microscope TCS SP2 (Leica, Bensheim, Germany) and an HCX PL APO 63×/1.32-0.6 oil objective. Laser intensities were adjusted to avoid any defects in the development of the embryo. Images were collected at 20-second or 45-second intervals over a period of 15-35 minutes and processed using Adobe Photoshop 7.0.

Table 1. RNAi experiments

Gene targeted	Sequence (5′–3′)	RNAi method
K09H11.3 (RhoGAP)	GTTACACTCTTGGAGAGGTATGCTC TGGACTCTTGGTTCTCTTCATATTC	Feeding, injection
K09H11.3 (middle)	CGAGAAATAACGGTAGTGGAAAGT GAGATTGGTTCTAGGAGACGATGT	Feeding
K09H11.3 (3 UTR)	GTTTAGTGCGATCCAGAGTCAAT TGCATTGAAGTTAAGAGATGGGTA	Feeding
Y75B7AL.4 (middle)	CGAGAATGTAAAATCCAGAAACG TTGGAGTGAGATTGGTTCT	Feeding
cyk-4 (Kamath et al., 2003)	TGGTTTGTCCTGGTGTTTGA ACGGTTTTCACGCATTTTTC	Feeding
cyk-4	GGTCGCAAGAAGCTGGCAAT TGGTTTGTCCTGGTGTTTGA	Feeding, injection
rho-1	ATTATGTTGCCGACATTGAAGTT CATGCACTTGCTCTTCTTTTTCT	Feeding, injection
cdc-42 (Kamath et al., 2003)	TTCTTCGATAATTATTGCTCCCA AACGACGACGAAAATGTTAAAGA	Feeding
cdc-42	AGATGGAGCTGTCGGTAAAACT TTCTTCTTCTTCTCCTGTTGTGG	Feeding, injection
let-502 (Kamath et al., 2003)	GCATTATCTCGATCACGGGT ATTTGAACTCCGACCGAATG	Feeding
nmy-2 (Kamath et al., 2003)	TCCGAGAAGTGAAGCGATTT TATGCAGAACGTCTCAACCG	Feeding
ect-2 (Kamath et al., 2003)	CTCTGAATTTCTGCCAAAGCC GGCAAAGAAATCCGATTCAA	Feeding, injection

The guide strands (top) and anti-guide stands (bottom) are shown.

Table 2. Penetrance of the ruffling phenotype and embryonic lethality in early embryos

	Ruffling phenotype (%)	Embryonic lethality rate (%)
rga-3/4(RNAi)	62.3 (*n*=131)	82.10
rga-3(RNAi)	26.5 (*n*=159)	9.30
rga-3 3′UTR(RNAi)	24.0 (*n*=54)	4.24
rga-4(RNAi)	42.2 (*n*=90)	6.36
cyk-4(RNAi)	2.8 (*n*=106)	22.75
Control	6.6 (*n*=106)	1.40

The penetrance of the ruffling phenotype was determined by imaging embryos from the one- to two-cell stage. *n* gives the number of embryos analyzed for each category. Control refers to embryos from mothers fed with empty pDT7 vector. Images of the representative embryos for each RNAi are shown in Fig. 2. The embryonic lethality rate was determined by counting the offspring of animals subjected to RNAi treatment in parallel experiments to those used for the determination of penetrance of the ruffling phenotype.

Quantification of the domain sizes of PAR-2 and PAR-6

ImageJ was used to measure the PAR-2 and PAR-6 domains in wild-type and RNAi-treated embryos. Pictures of embryos – from the beginning of polarization until reaching the two-cell stage – were acquired in the Nomarski and the GFP channel. For quantification, the length of the embryo was measured by drawing a line from the anterior to the posterior of the embryo with ImageJ; this line was set to 100%. The length of the respective PAR domain was measured along this line by using the cortical GFP localizations. The ratio between the length of the PAR domain and the length of the entire embryo was determined.

Quantification of GFP::NMY and GFP::RHO-1 signals

To quantify the GFP signals in wild-type and *rga-3/4(RNAi)* embryos, either confocal or epifluorescence pictures with the same exposure times were subjected to analysis with ImageJ. The length of NMY-2::GFP patches in the embryo before pronuclear meeting was determined by drawing cortical lines corresponding to the contractile patches with the highest fluorescence signal. The length of these lines was measured.

For quantification of the RHO-1::GFP data, the cortical fluorescence signal was measured. The ratio of the signal between the contractile cortex at the ingressing furrow and the non-contractile cortex was determined.

DAPI and rhodamin-phalloidin staining of gonads

Young adult worms were cut open to release the gonads in a depression slide and gonads were fixed with 3.7% formaldehyde for 10 minutes at room temperature. After washing with egg buffer, incubation in 0.4% BSA, 0.1% Tween-20 for 10 minutes, followed by another washing step, the gonads were stained with rhodamin-phalloidin (Molecular Probes, 0.01 U/μl) and DAPI (Boehringer Mannheim, 0.5 μg/ml) in a wet chamber for 30 minutes at room temperature. Gonads were mounted onto an agarose pad and examined with a Zeiss Axioplan 2 microscope using a 40× Axioplan objective as described above.

RESULTS

Two RhoGAP proteins are required to control membrane ruffling in the early *C. elegans* embryo

Upon fertilization, the *C. elegans* zygote segregates specific proteins and RNAs to opposite poles to provide asymmetry and polarity for the subsequent cell division (Schneider and Bowerman, 2003). This polarity establishment involves cytoplasmic streaming and cortical contractions. The nature of the membrane dynamics and the cortical contractions upon fertilization are poorly understood. Therefore, we undertook a candidate approach and screened databases for genes that influenced membrane dynamics, especially cortical movement and membrane ruffling in the fertilized *C. elegans* oocyte. RNAi of K09H11.3 resulted in a pronounced increase in membrane ruffling and ectopic furrowing after fertilization, and increased pseudo-cleavage (Fig. 1A,B; compare Movies 1 and 2 in the supplementary material), similar to phenotypes that had been reported previously (Kamath et al., 2003; Simmer et al., 2003; Sonnichsen et al., 2005). The membrane dynamics in the RNAi embryos were strongly increased compared with wild type and the pseudo-cleavage was sometimes shifted towards the anterior pole. Upon RNAi, the number of ruffles increased at least two- to threefold over wild type (Fig. 1B). The depth of the ruffles was also increased [*rga-3/4 (RNAi)*: 6.32±2.0

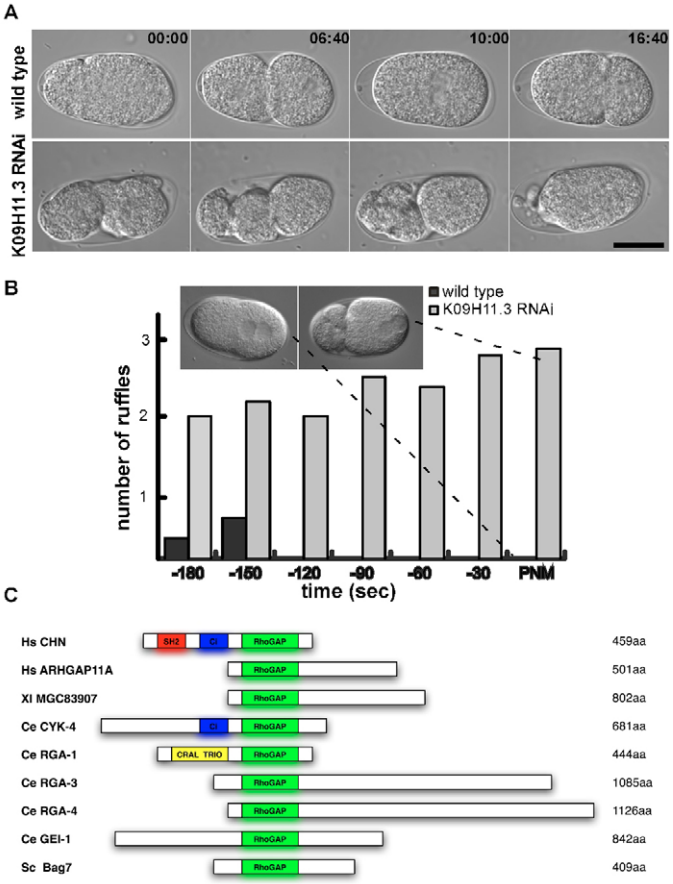

Fig. 1. The RhoGAP protein K09H11.3 is required to control membrane ruffling in the early *C. elegans* embryo. (**A**) Pictures from time-lapse studies of wild-type and K09H11.3 RNAi-treated embryos. K09H11.3 RNAi treatment was performed by feeding dsRNA-expressing bacteria targeting the RhoGAP domain containing the N-terminus of the K09H11.3 gene (*rga-3*). Embryos are grown at 20°C and mounted for microscopy: anterior ruffling is more pronounced in the RNAi-treated embryo (lower panel) than in the wild-type embryo (upper panel). This exaggerated ruffling also persists longer in the RNAi-treated embryo than in wild type. (**B**) Quantification of ruffles in embryos up to pronuclear meeting (PNM) in wild type (*n*=8) and after K09H11.3 RNAi treatment (*n*=13). The ruffles were counted from time-lapse movies of individual embryos. The average number of ruffles per embryo at a given time point is indicated. (**C**) Schematic drawing of different RhoGAP-domain-containing proteins in humans (hs), *Xenopus laevis* (Xl), *C. elegans* (Ce) and *Saccharomyces cerevisiae* (Sc). The RhoGAP domain (green) is present in most RhoGAPs in the more C-terminal part of the protein. RGA-3 and RGA-4 belong to a family of uncharacterized RhoGAP-domain proteins, which carry the GAP domain at the N-terminus of the protein. The SH2 domain, the C1 domain and the CRAL/Trio domain are depicted in red, blue and yellow, respectively. Scale bar: 20 μm.

μm; wild type: 3.24±1.57 μm). Most importantly, ruffles formed until pronuclear meeting, which was not the case in wild type (Fig. 1B). Sequence analysis revealed, however, that another gene, Y75B7AL.4, which is 81% identical to K09H11.3 on the amino acid level, was probably also reduced upon RNAi treatment, because our RNAi construct – like those used in other screens – targeted the highly conserved 5′ region of the K09H11.3 transcript (see Fig. S1 in the supplementary material). Both genes encode putative RhoGAP proteins that accelerate GTP hydrolysis on members of the Rho family, namely on RHO, CDC42 and RAC (Fig. 1C). K09H11.3 and Y75B7AL.4 were named RGA-3 and RGA-4 for RhoGAP-3 and RhoGAP-4, respectively. RGA-1 and RGA-2 are RhoGAPs expressed in epithelial cells and are the worm orthologues of mammalian RhoGAP1 (ARHGAP1) and ARHGAP20, respectively (Jenna et al., 2005; Schwarz et al., 2006). RGA-3 and RGA-4 belong to a subfamily of RhoGAPs with their GAP domain located at the N-terminus. Other members of this family comprise the hitherto uncharacterized mammalian ARHGAP11A and the amphibian MGC83907 (Fig. 1C). Both RGA-3 and RGA-4 are expressed in the germ line and in the early embryo (NEXTDB Version 4.0). Expression seems to cease for both genes around the 100- to 200-cell stage. These are not the only RhoGAPs expressed at this early stage: CYK-4 is essential for cytokinesis and polarity establishment in the P0 cell (Jantsch-Plunger et al., 2000; Jenkins et al., 2006). RNAi treatment of CYK-4 generated multinucleated cells because of cytokinesis failure (Jantsch-Plunger et al., 2000) and cortical anterior markers were distributed over the entire cortex (Jenkins et al., 2006).

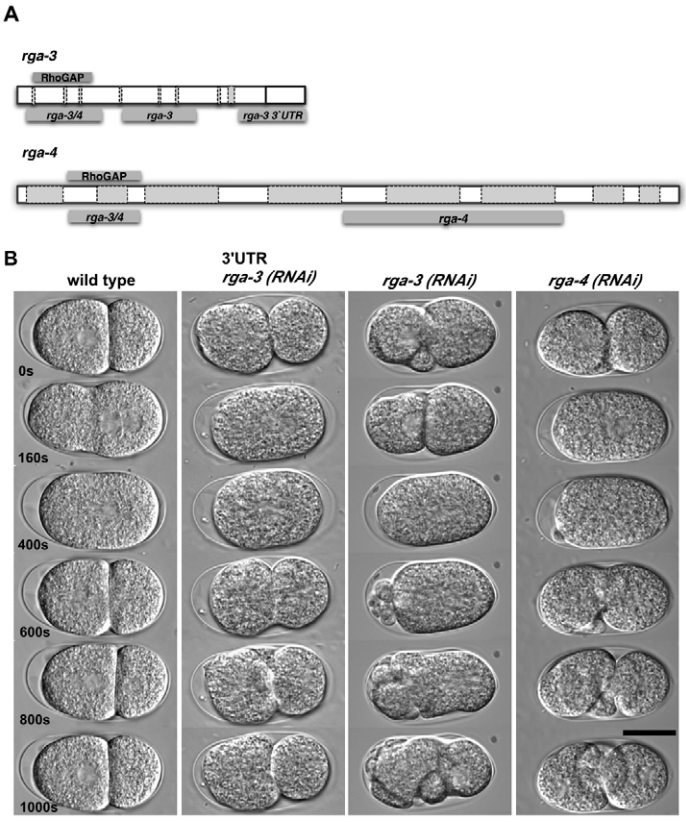

Fig. 2. Knockdown of either RGA-3 or RGA-4 leads to a hyper-contractile cortex. (**A**) Schematic drawing of the RNAi constructs used: for *rga-3*, apart from the initially cloned N-terminal sequence, constructs matching the middle part and to the 3′UTR of the gene are chosen; for *rga-4*, an RNAi targeting the middle part of the gene is also created. Exons are indicated in white stretches; introns in yellow. Introns are bigger in the Y75B7AL.4 gene (*rga-4*) compared to K09H11.3 (*rga-3*). (**B**) Pictures of Nomarski time-lapse studies after feeding with bacteria expressing dsRNA of the different RNAi constructs. For all constructs, a membrane-ruffling phenotype was observed. s, seconds. Scale bar: 20 μm.

RGA-3 and RGA-4 have overlapping functions in the early *C. elegans* embryo

To decipher the contribution of RGA-3 and RGA-4 to the membrane-ruffling phenotype, we constructed different RNAi probes specifically targeting either RGA-3 or RGA-4 (Fig. 2A). Knockdown of the individual genes caused, in both cases, cortical hyper contractility, albeit with a lower penetrance (Table 2, Fig. 2B). Thus, RGA-3 and RGA-4 have overlapping functions and, given the phenotype of the RNAi-treated worms, both RhoGAPs are involved in inactivation of a Rho family GTPase, most probably at the plasma membrane. The contraction phenotypes were additive and the loss of both GAPs resulted in embryonic lethality, indicating that these two proteins are at least partially redundant. By contrast, another early-expressed RhoGAP, CYK-4, either plays less of a role or is not involved in the same process, because no anterior ectopic furrowing or invaginations were observed when this GAP was knocked down, although cytokinesis failures were detected (Tables 2 and 4). Given the redundant function of RGA-3 and RGA-4, the N-terminal construct, which targets both proteins and resulted in the highest penetrance, was therefore used for all subsequent experiments.

Loss of RHO-1 function rescues the ruffling phenotype of *rga-3/4(RNAi)*

Which Rho GTPase is regulated by RGA-3/4? Lack of RGA-3/4 GAP activity leads to sustained activation of its target GTP-binding protein. In the early embryo, two GTPases of the Rho family show severe phenotypes when knocked down by RNAi: RHO-1 (the orthologue of mammalian RhoA) and CDC-42. Both GTPases have been reported to control actin dynamics in numerous different cell types and organisms (Narumiya and Yasuda, 2006; Raftopoulou and Hall, 2004). In the early *C. elegans* embryo, however, they seem to also be essential for the establishment and maintenance of polarity (Motegi and Sugimoto, 2006; Schonegg and Hyman, 2006; Gotta et al., 2001; Kay and Hunter, 2001). Upon knockdown of the specific GTPase regulated by the RhoGAPs, the hyper-contractility phenotype should be rescued, because the GTPase would no longer be present to hyper-activate the acto-myosin network, which performs the contractions in the early embryo. By contrast, if the GTPase were not involved in the regulation of the acto-myosin system at the anterior cortex, loss of this specific GTPase activity would have no impact on the ectopic furrowing and membrane ruffling. Whereas RNAi of RHO-1 rescued the extensive-ruffling phenotype caused by knockdown of RGA-3/4, reducing the levels of CDC-42 had no effects on the extent of invaginations and contractions (Fig. 3A,B, Movies 3-6, Table 3). CDC-42 levels were reduced in the triple-RNAi experiment, because polarity defects were observed as described for *cdc42(RNAi)* (Gotta et al., 2001; Kay and Hunter, 2001). More importantly, no cortical contractions were observed at all upon *rho-1(RNAi)*, indicating that RHO-1 is responsible for the regulation of the acto-myosin network at the anterior cortex. RHO-1 has been implicated in the control of all contractions at the cortex (Motegi and Sugimoto, 2006; Schonegg and Hyman, 2006). Our results strongly indicate that RGA-3/4 act as RhoGAPs on RHO-1 and that they control contractility at the anterior cortex.

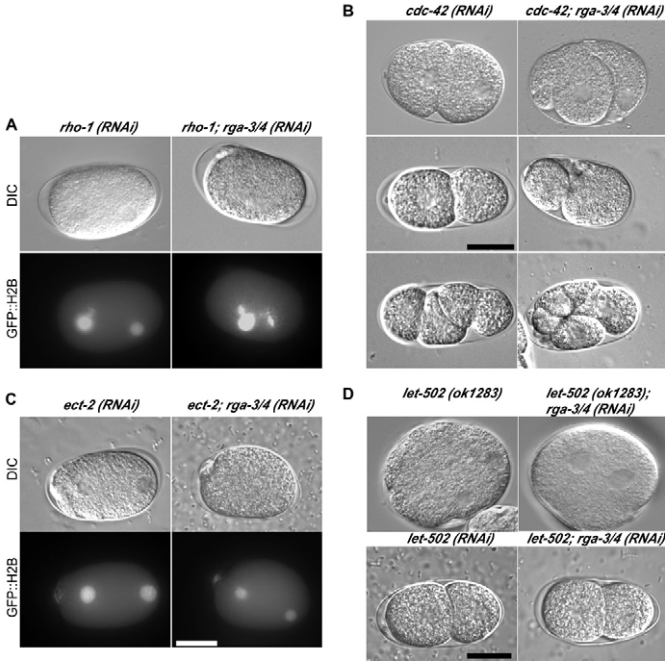

Fig. 3. RGA-3 and RGA-4 are RhoGAPs for RHO-1 and not for CDC-42. (**A-D**) Epistasis RNAi experiments of *rho-1* (A), *cdc-42* (B), *ect-2* (C) or *let-502* (D) with or without *rga-3* and *rga-4* (*rga-3/4*) were performed by feeding with the RNAi construct in question either alone, or by mixing together the same amounts of bacteria containing the *rga-3/4* construct or RNAi construct being studied and feeding these at the same time. In the case of LET-502, epistasis experiments were also performed with the *let-502(ok1283)* allele, which is a knockout of LET-502. (A) Concomitant knockdown of RGA-3/4 and RHO-1 led to a catastrophic one-cell arrest, similar *to rho-1* RNAi treatment [*rho-1(RNAi)*]. (B) *cdc-42(RNAi)* did not rescue the *rga-3/4(RNAi)* phenotype. The knockdown of the RhoGEF ECT-2 (C) and the Rho-associated kinase LET-502 (D) rescued the *rga-3/4(RNAi)* phenotype. Nuclei were visualized with GFP::H2B. Scale bars: 20 μm.

To provide further evidence in support of this hypothesis, we simultaneously knocked down the GEF for RHO-1, ECT-2, with RGA-3/4 (Fig. 3C, Table 3). Again, the membrane-ruffling phenotype was rescued and contractility was greatly reduced even when compared to wild type. Without its GEF, RHO-1 cannot be activated and thus the concomitant loss of the GAPs has no impact on the phenotype. Finally, we knocked down the RHO-1-associated kinase (ROCK), which, in *C. elegans*, is encoded by *let-502* and relays the signal of RHO-1 to the acto-myosin network (Piekny and Mains, 2002). As predicted, co-knockdown of ROCK and RGA-3/4 rescued the cortical hyper-contractility caused by the loss of RGA-3/4 function. Furthermore, knockdown of RGA-3/4 in *let-502*$^{-/-}$ animals gave a similar result (Fig. 3D, and see Movies 7 and 8 in the supplementary material).

GFP::RHO-1 is enriched at the plasma membrane in *rga-3/4(RNAi)* embryos

To determine the effect of silencing GAP expression on the subcellular distribution of the Rho GTPase, we localized GFP::RHO-1 in wild-type and *rga-3/4(RNAi)* embryos. In wild type, RHO-1 was mostly cytoplasmic but was also visible at the cortex. Upon loss of RGA-3/4, GFP::RHO-1 was enriched at the plasma membrane, more precisely in the ruffles and furrows (Fig. 4). We

Table 3. Quantification of phenotypes of the epistasis experiments

	Cytokinesis (*rho-1*, *ect-2* and *nmy-2*) or polarity (*cdc-42*) defective (%)	Exaggerated ruffling (%)
rho-1(RNAi)	66 (*n*=39)	nd
rho-1;rga-3/4(RNAi)	66 (*n*=39)	12.0 (*n*=39)
ect-2(RNAi)	80 (*n*=30)	nd
ect-2;rga-3/4(RNAi)	48 (*n*=45)	8.0 (*n*=45)
cdc-42(RNAi)	32 (*n*=31)	nd
cdc-42;rga-3/4(RNAi)	7 (*n*=27)	59.0 (*n*=27)
nmy-2(RNAi)	54 (*n*=31)	nd
nmy-2;rga-3/4(RNAi)	41 (*n*=46)	8.8 (*n*=46)

The phenotype in RNAi experiments was determined by analyzing F1 embryos derived from mothers subjected to RNAi. Cytokinesis failure was used as a read-out for *rho-1*, *ect-2* and *nmy-2* RNA treatment (*RNAi*) phenotypes, whereas polarity defects (as judged by parallel cleavages of AB and P1, see Fig. 3C) was counted as a read-out for the *cdc-42(RNAi)* phenotype. Exaggerated ruffling was judged as shown in Fig. 2. RNAi was performed either by injection or feeding. *n* is the number of embryos per condition analyzed. nd, not determined.

determined the ratio of the concentration of RHO-1 at a given length at the contractile and at the non-contractile cortex in wild-type and *rga-3/4(RNAi)* embryos. The ratio in the RNAi-treated embryos was higher (1.55±0.21; n=11) compared with wild type (1.34±0.12; n=9; P<0.05). Given the increased number and persistence of ruffles in the knockdown, this ratio even underscores the enrichment of GFP::RHO-1 at the plasma membrane in *rga-3/4(RNAi)* zygotes. This result is exactly what one would expect for a GTPase that can no longer be deactivated and cannot stop signalling downstream. Therefore, the enrichment of GFP::RHO-1 in the ectopic cleavage furrows at the plasma membrane substantiates our finding that RGA-3/4 act on RHO-1. Taken together, these experiments strongly indicate that RGA-3/4 are novel RhoGAPs for RHO-1 during early embryonic development and that they regulate contractility at the anterior cortex.

RGA-3/4 function is not required for proper cytokinesis

RHO-1 and CDC-42 are both involved in cytokinesis. Therefore, by co-staining early embryos with the lipophilic dye FM4-64 and GFP::H2B, we investigated whether *rga-3/4(RNAi)* causes cytokinesis defects. FM4-64 served as a marker for the plasma membrane in these experiments. *rga-3/4(RNAi)* resulted in a moderate cytokinesis defect (Table 4 and see Fig. S2 in the supplementary material). Upon feeding, approximately 20% of the *rga-3/4(RNAi)* embryos showed multinucleated and anucleated cells. We observed cytokinesis defects, which were most probably a result of extra furrowing, that led to small anucleate cells (see Fig. S2 in the supplementary material). However, injection of RGA-3/4 dsRNA yielded in a higher level of over-pronounced cleavages and less cellularization defects (Table 4). Therefore, we concluded that failure in cytokinesis upon *rga-3/4(RNAi)* is most likely a secondary effect and that RGA-3/4 play no major role in cytokinesis.

The non-muscle myosin NMY-2 is enriched at the anterior cortex after *rga-3/4(RNAi)*

The extensive contractility and ruffling caused by loss of RGA-3/4 function implied a role for actin and the non-muscle myosin NMY-2 (Guo and Kemphues, 1996) in this process. To test whether NMY-2 acts downstream of RGA-3/4-dependent RHO-1, we first knocked down both NMY-2 and RGA-3/4 (Fig. 5A). The ruffling phenotype of *rga-3/4(RNAi)* was rescued by the simultaneous loss of NMY-2

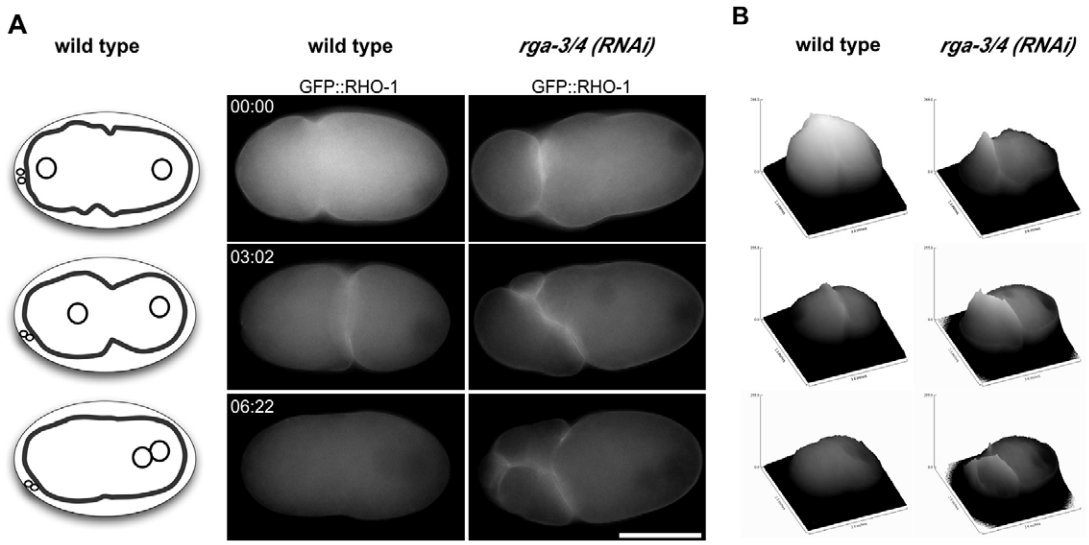

Fig. 4. GFP::RHO-1 accumulates at ingressing furrows in *rga-3/4(RNAi)* embryos. (**A**) Pictures from time lapses showing GFP::RHO-1 in wild-type or *rga-3/4(RNAi)* embryos. The different stages are depicted in the cartoon. (**B**) Visualization of GFP intensities in the respective embryos using ImageJ. Scale bar: 20 μm.

and RGA-3/4 function, confirming that indeed the contractile machinery in the early embryo is hyper-activated in the absence of the GAPs RGA-3/4. Hence, NMY-2::GFP should be enriched at the anterior cortex in *rga-3/4(RNAi)* embryos, which was what we observed: NMY-2::GFP was concentrated in invaginations and ectopic cleavages in the anterior part of *rga-3/4(RNAi)* embryos as well as in the pseudo-cleavage (Fig. 5B,C). Moreover, NMY-2::GFP covered a large extent of the anterior cortex, unlike the NMY-2::GFP speckles detected in wild-type embryos before pronuclear meeting (Fig. 5B-D). The NMY-2 patches at the cortex were at least twice as long in *rga-3/4(RNAi)* than in wild-type embryos (Fig. 5D). The concentration of NMY-2::GFP was also strongly increased in the cleavage furrow of the first cell division after RGA-3/4 knockdown (data not shown). Thus, the inability of the embryo to deactivate RHO-1 at the anterior cortex results in hyper-activation and aberrant recruitment of the acto-myosin system to the cortex.

Onset of polarity occurs normally in *rga-3/4(RNAi)* embryos

After fertilization and meiosis II of the female pronucleus, the entire cortex of the embryo is contractile. Via the cortical and cytoplasmic streaming, ruffling later becomes restricted to the anterior part of the embryo. These contractions and ruffles are thought to be important for the establishment of polarity in the early embryo. In a subset of *rga-3/4(RNAi)* embryos, extensive ruffling and furrowing was not restricted to the anterior part and seemed to extend also towards the posterior region of the embryo. Therefore, we wanted to determine whether polarity establishment occurred normally upon depletion of RGA-3/4. First, we tested whether posterior polarity was established in *rga-3/4(RNAi)* embryos in the same manner as in wild type. Despite the extensive ruffling, the polarity establishment seemed to be mostly correct and we did not detect a significant difference in the posterior cortex area upon *rga-3/4(RNAi)* compared to wild type, as judged by the localization of the posterior marker GFP::PAR-2 (Fig. 6A,C). Because the ruffling in wild type occurs at the anterior cortex, we next tested the localization of GFP::PAR-6 in *rga-3/4(RNAi)* embryos. PAR-6 normally localizes together with PAR-3 and the atypical PKC, PKC-3, to the anterior cortex (Hung and Kemphues, 1999). Again, the onset of polarity was unperturbed. However, the GFP::PAR-6 signal seemed to be restricted to the hyper-contractile region and within the cleavage furrow (Fig. 6B and see Movie 9 in the supplementary material).

Taken together, our data indicate that there is no primary defect in polarity onset and maintenance per se. However, we observed greater fluctuations in the anterior-domain size as signified by GFP::PAR-6, indicating that the stable posterior domain prevented overshooting of the anterior domain into the posterior part of the embryo (Fig. 6C). Conversely, knockdown of the other GAP, CYK-4, caused a polarity defect, because GFP::PAR-6 and NMY-2::GFP could be detected over the entire cortex and GFP::PAR-2 was mostly cytoplasmic (Jenkins et al., 2006) (Fig. 7, Table 4 and see Movie 10 in the supplementary material). The fact that knockdown of RGA-

Table 4. Quantification of phenotypes after RhoGAP RNAi

	Cytokinesis defective		
	Cellularization failure (%)	Over-pronounced cleavages (%)	Polarity defective (%)
cyk-4(RNAi)	94 (*n*=18)	0 (*n*=18)	65.0 (*n*=20)
rga-3/4(RNAi)	0 (*n*=20)	65 (*n*=20)	18.5 (*n*=27)
cyk-4;rga-3/4(RNAi)	54 (*n*=33)	42 (*n*=33)	70.1 (*n*=24)
Control	0 (*n*=18)	0 (*n*=18)	0.0 (*n*=18)

The phenotype was determined by analyzing F1 embryos derived from mothers subjected to RNAi. Control represents wild-type embryos from mothers fed with OP50 bacteria. Cytokinesis failure was classified into either furrow-regressing failure ('cellularization failure') and therefore arrest as multinucleated embryos or 'over-pronounced cleavages' as indicated by extra furrows built during first cell division (Fig. 2; 1000s). The polarity phenotype was scored by the localization of PAR-2 and PAR-6 after the first mitosis of the embryo. *n* is the number of analyzed embryos. RNAi was performed by injection or soaking.

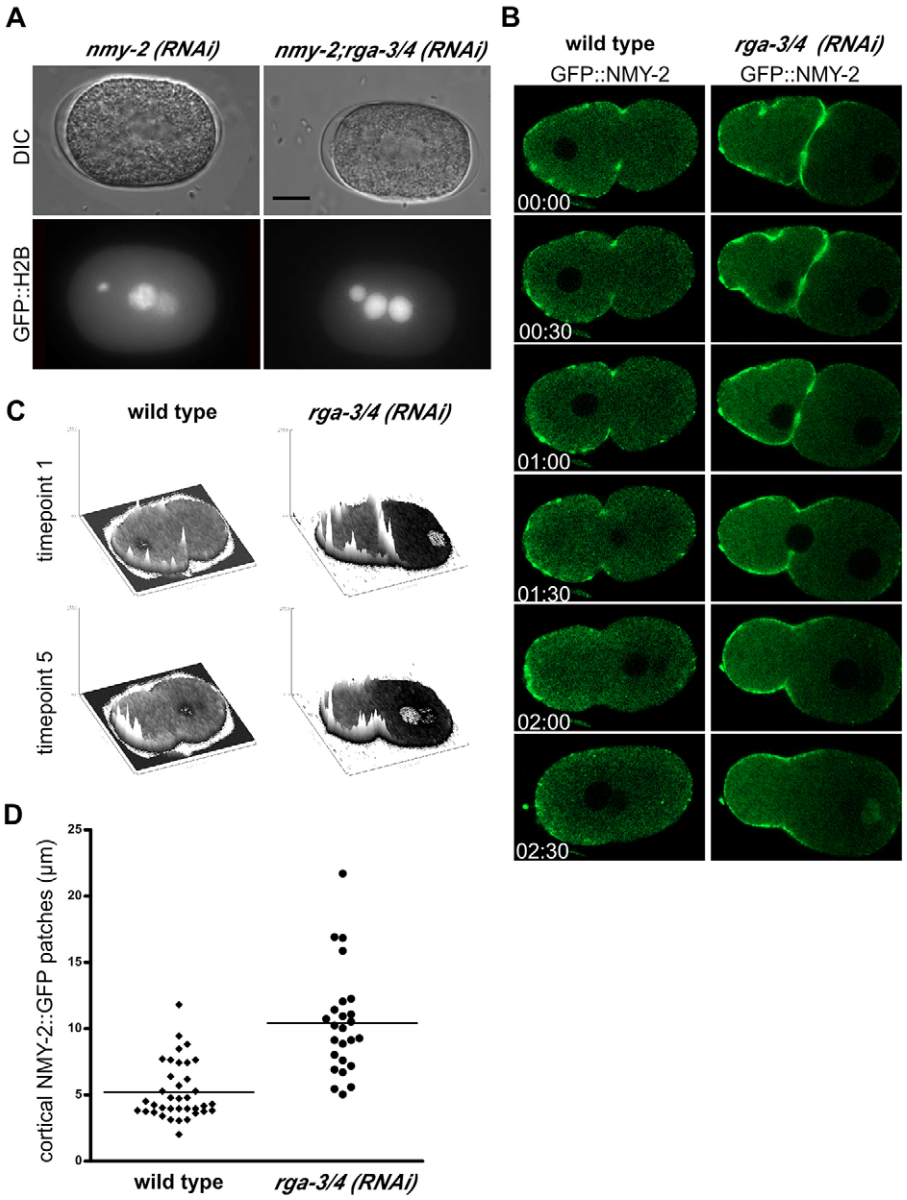

Fig. 5. Hyper-contractility in *rga-3/4(RNAi)* embryos is dependent on NMY-2, and NMY-2::GFP is enriched at cortical membrane ruffles in *rga-3/4(RNAi)* embryos. (**A**) *nmy-2(RNAi)* rescues the membrane-ruffling defect of *rga-3/4(RNAi)*. All three proteins were knocked down at the same time by feeding. (**B**) Time-lapse images of NMY-2::GFP behaviour in wild-type and *rga-3/4(RNAi)* embryos. NMY-2::GFP is strongly enriched in the pseudo-cleavage furrow and at the anterior cortex after *rga-3/4(RNAi)*. (**C**) Quantification of the fluorescence intensity of NMY-2::GFP using ImageJ. (**D**) Quantification of the length of the NMY-2::GFP domains at the plasma membrane in wild-type (n=7) and *rga-3/4(RNAi)* (n=9) zygotes. Scale bar: 20 µm.

3/4 did not cause any major polarity defects suggests that the GAPs fulfil different functions in the early embryo. If this were the case, the phenotypes caused by the loss of the three GAPs should lead to extended membrane ruffling and to a polarity defect. When we performed simultaneous knockdown of the three GAPs, we observed a hyper-contractile cortex [caused by the *rga-3/4(RNAi)*], and NMY-2::GFP was spread over the entire cortex and GFP::PAR-2 was cytoplasmic, indicating a loss of polarity [caused by the *cyk-4(RNAi)*] (Fig. 7). Furthermore, we detected a strong cytokinesis defect unlike the effect we observed upon *rga-3/4(RNAi)* (Table 4). Hence, CYK-4 and RGA-3/4 appear to fulfil different functions in the P0 cell.

A role for RGA-3/4 in the germ line

To gain insight into the subcellular localization of RGA-3, we expressed a GFP::RGA-3 fusion in the germ line under the control of the *pie-1* promoter. The expression of GFP::RGA-3 seemed to be toxic, because it was very difficult to obtain and maintain transgenic lines. Furthermore, the transmission of the extrachromosomal array was very poor, the transgenic worms had a reduced brood size and only a few offsprings contained the transgene. Given these difficulties, it was impossible to analyze the early embryonic phenotype in a quantitative manner. However, in adult transgenic animals, we observed robust defects in gonad proliferation and migration, whereas the gonad architecture seemed to be unaffected (see Fig. S3 in the supplementary material, data not shown). Gonad arms were too long and crossed from one side of the body to the other. GFP::RGA-3 was barely detectable in the gonad, which might be due to low expression because of germline silencing of the transgene.

We inferred from our studies in the zygote that RGA-3/4 are involved in the control of the *C. elegans* ROCK, LET-502, and given the phenotype of the expression of GFP::RGA-3, we tested the effect of RGA-3/4 RNAi treatment on the temperature-sensitive (ts) *let-502(sb106)* mutant in the germ line. Although *let-502*$^{-/-}$ animals are sterile and have severe gonadal defects, such as unusually large spaces devoid of nuclei and actin (‘holes’), or nuclei fallen into the rachis, the ts mutant *let-*

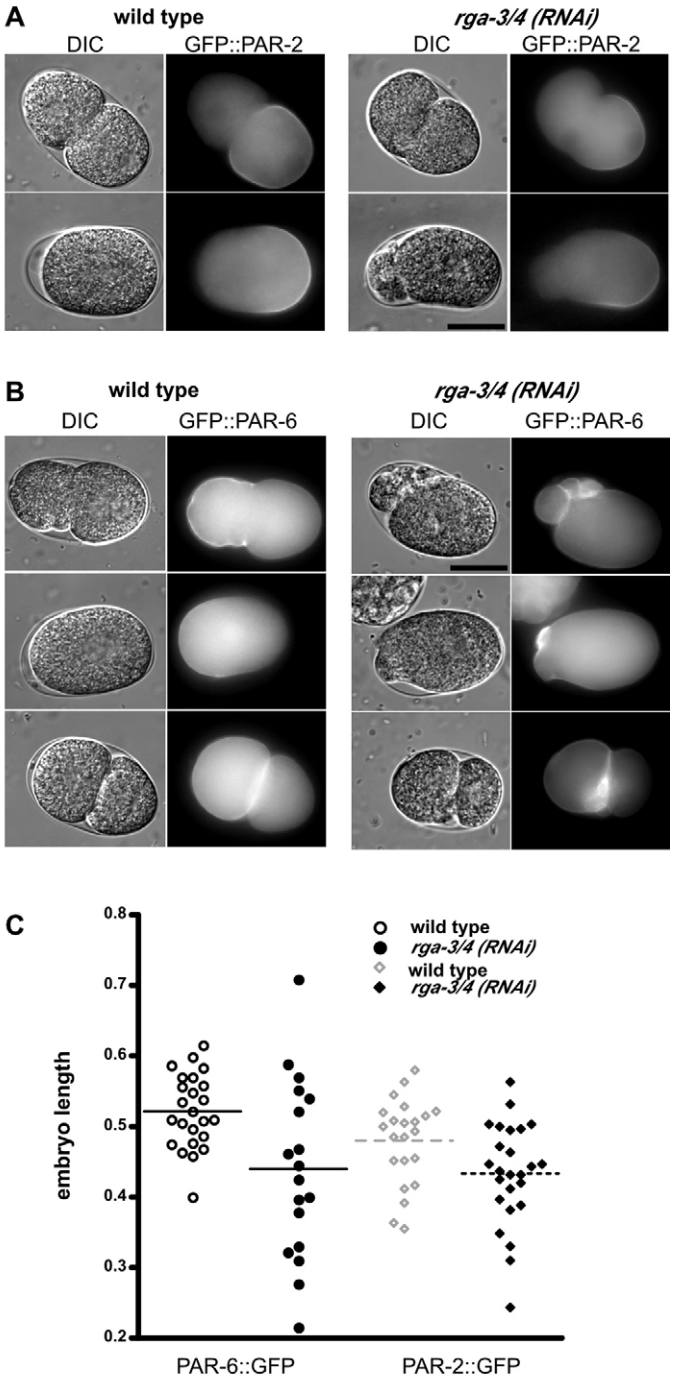

Fig. 6. Polarity establishment is not affected in *rga-3/4(RNAi)* embryos but the anterior PAR-6-domain size fluctuates more in *rga-3/4(RNAi)* embryos compared with wild type. (**A**) GFP::PAR-2 and (**B**) GFP::PAR-6 localization is determined in vivo in wild-type and in *rga-3/4(RNAi)* embryos. GFP::PAR-2 as well as GFP::PAR-6 is correctly localized in *rga-3/4(RNAi)* embryos at the posterior and anterior cortex, respectively. (**C**) The relative size of the GFP::PAR-2 (wild type: n=24 embryos; RNAi: n=18) and GFP::PAR-6 (wild type: n=22; RNAi: n=25) domains was determined by drawing a line from the anterior to the posterior end of the embryo and then measuring the size of the individual domain. The size of the GFP::PAR-6 domain fluctuated more in *rga-3/4(RNAi)* embryos, compared with wild type. The variations in the domain sizes are statistically significant ($P<0.01$). The size of the GFP::PAR-2 domain was less affected. Scale bars: 20 μm.

502(sb106) showed barely any gonadal defects at the restrictive temperature of 23°C (Fig. 8A,B). Knockdown of RGA-3/4 aggravated the *let-502(sb106)* phenotype such that the gonadal defects were very similar to those observed in *let-502*$^{-/-}$ animals; 'holes' and strong defects in distal and proximal rachis formation were observed. Conversely, *rga-3/4(RNAi)* by itself had no effect on gonad migration or brood size (Fig. 8A,C). The only noticeable phenotype was a problem in the formation of the distal rachis. A similar, mild gonad defect was observed upon *cyk-4(RNAi)*. However, no enhancement of the gonad phenotype was observed in *let-502(sb106)* mutants. Taken together, our data suggest a role for RGA-3/4 as GAPs for RHO-1 in the germ line and in the early embryo, and that these functions might be, at least in part, temporally and spatially distinct from the functions of CYK-4.

DISCUSSION

We have identified two novel RhoGAPs, RGA-3/4, that are essential to turn off RHO-1 signalling to the acto-myosin network at the anterior cortex in the *C. elegans* zygote. Furthermore, RGA-3/4 are required for proper germline formation. The two novel RhoGAPs belong to an uncharacterized subfamily. They carry the GAP domain at the N-terminus and the remainder of the proteins do not contain any known interaction or signalling motifs, which is unusual for RhoGAP proteins (Jaffe and Hall, 2005; Moon and Zheng, 2003). The two vertebrate orthologues, the mammalian ARHGAP11A and the amphibian MGC83907, have the same domain structure and also lack known motifs, and might therefore fulfil similar functions. How do these proteins interact with effector molecules or provide specificity for Rho GTPases? It seems rather likely that these GAPs contain yet unidentified interaction domains. Further analysis of this novel class of regulators is likely to reveal interesting and new roles for Rho during development.

In *C. elegans*, RGA-3/4 are expressed in the germ line and in the early embryos, probably up to the 100- to 200-cell stage [Nematode Expression Pattern DataBase (NEXTDB), Ver. 4.0]. Another RhoGAP, CYK-4, is expressed in a similar pattern. Although these GAPs are expressed in the same cells, and target the same GTPase, their biological functions are largely non-overlapping. RGA-3/4 seem to control the contractility of the acto-myosin network, whereas CYK-4 is involved in cytokinesis, and in polarity establishment and maintenance (Jenkins et al., 2006) (Fig. 7 and Table 4). By contrast, RGA-3/4 do not seem to play any primary role in meiosis, mitosis, polarity establishment or cytokinesis. The occasional failure in these processes upon *rga-3/4(RNAi)* might be due to the destruction or compromised assembly of cellular structures by the extensive furrowing and the hyper-contractility. Polarity setup and maintenance were also mostly normal. We observed, however, a significant fluctuation in the size of the GFP::PAR-6 domain, indicating that the boundaries separating the anterior and posterior domains might not be stable. RGA-3/4 clearly control contractility-related functions of RHO-1, and seem to be specific for this process. However, the bulk of CYK-4 is located at the mitotic spindle and only some paternal CYK-4 is found at cortex at the sperm entry site (Jantsch-Plunger et al., 2000; Jenkins et al., 2006).

Three RhoGAPs expressed in the germ line have been characterized so far: CYK-4, and now RGA-3/4; all of which act on RHO-1. No GAP for CDC-42 in the early *C. elegans* embryo has been identified yet. However, CYK-4 and RGA-3/4 act on RHO-1, which is upstream of CDC-42 in the zygote. Therefore, despite the result of the epistatic analysis, we cannot rule out that one or more of the three GAPs also turns off CDC-42. Another

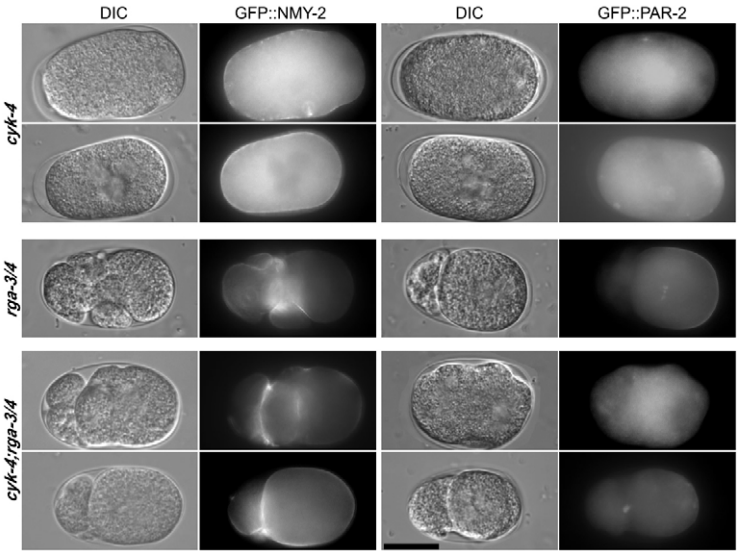

Fig. 7. CYK-4 and RGA-3/4 fulfil different functions in the early *C. elegans* embryo. To compare the functions of the three RhoGAPs – RGA-3/4 and CYK-4 – present in the early embryo, RNAi epistasis experiments were performed by injecting dsRNA into the embryos. Whereas CYK-4 was essential for the first division and to recruit GFP::PAR-2 to the posterior cortex (upper panels), RGA-3/4 played a role in downregulating contraction (middle panels). Simultaneous knockdown of all three RhoGAPs resulted in a combination of both phenotypes; embryos did not undergo cytokinesis, the cortex remained contractile and NMY-2 spread over the entire cortex (lower panels). Scale bar: 20 μm.

possibility is the presence of at least one other GAP, which is likely to be the case (NEXTDB, Ver. 4.0). But why would we need so many different RhoGAPs? Perhaps the GAPs provide the specificity for Rho activity (Moon and Zheng, 2003) and hence provide the basis for temporal and spatial control of RHO-1 activity. This concerted action by the GAPs might be extremely important because there is only one RhoGEF expressed in the *C. elegans* zygote.

The RhoGEF ECT-2 might be the first target of the polarity cue provided by the sperm (Jenkins et al., 2006; Motegi and Sugimoto, 2006). Then, ECT-2 activates RHO-1, which in turn leads to the rearrangement of the acto-myosin network. To control the contractions performed by the acto-myosin network, the RhoGAPs RGA-3/4 inactivate RHO-1. If RHO-1 cannot be inactivated at the anterior cortex, cytoplasmic and cortical streaming still occurs, and therefore polarity establishment and maintenance are normal.

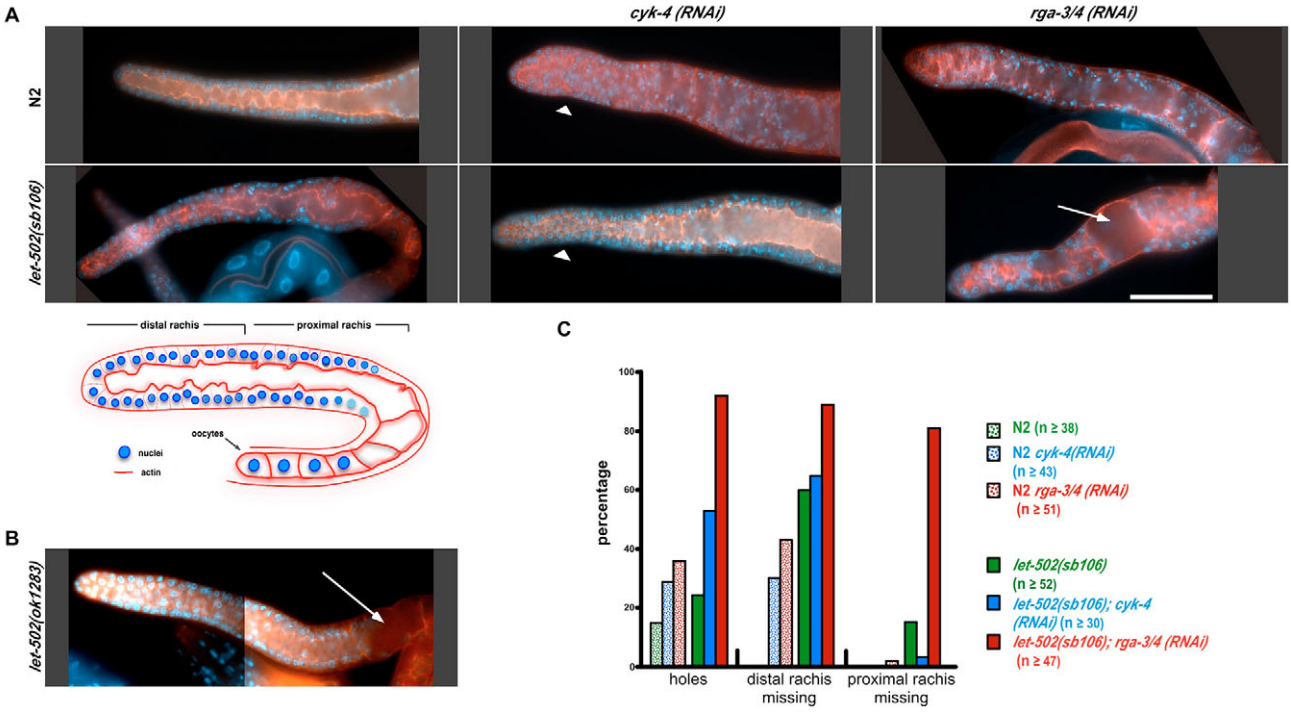

Fig. 8. *rga-3/4(RNAi)* causes strong gonad defects in *let-502(sb106)* mutants. (**A**) Gonad arms were extracted from worms and stained with rhodamin-phalloidin and DAPI. The gonads are oriented with the distal tip pointing towards the left. A schematic drawing of the gonad is included. The arrowheads point to the rachis formation defects. The arrow points to the 'hole' in the *let-502(sb106) rga-3/4(RNAi)* gonad. (**B**) A gonad from the *let-502(ok1283)* mutant, which represents a knock-out allele, was stained as in A. The arrow points to the 'hole'. (**C**) Quantification of gonad defects of N2 and *let-502(sb106)* animals treated with *rga-3/4* or *cyk-4* dsRNA. The number of gonads used for quantification of a particular phenotype is given in parenthesis. Depending on how the gonads adhered to the glass surface, not all phenotypes could be quantified in the same gonad. Ambiguous-looking gonads were not included in the analysis. Scale bar: 50 μm.

Motegi and Sugimoto suggested that CDC-42 maintains polarity by controlling the acto-myosin network in a second phase in the one-cell embryo (Motegi and Sugimoto, 2006). Our data are in agreement with this interpretation, because after centration, the entire cortex becomes smooth even upon *rga-3/4(RNAi)*, before the anterior part starts to contract again during cytokinesis. Therefore, CDC-42 still functions normally in the absence of RGA-3/4. CDC-42 might be involved in turning off RHO-1 signalling at the cortex during centration, perhaps by interacting with a RhoGAP. This GAP would be different from RGA-3 or RGA-4, because cortical ruffling stopped at centration upon loss of RGA-3/4 function. Interestingly, the original *cyk-4* mutant displayed less-pronounced furrowing, which is the opposite phenotype than that observed after *rga-3/4(RNAi)* (Jantsch-Plunger et al., 2000).

A possible scenario for the control of RHO-1 function is that first, upon fertilization, CYK-4 initiates cytoplasmic and cortical streaming, allowing the establishment of polarity. In a second step, RGA-3/4 control membrane contractility and the pseudo-cleavage at the anterior cortex by keeping RHO-1 activity at a certain threshold. Finally, CYK-4 takes over again; however, this time at the mitotic spindle, where CYK-4 controls cytokinesis. This rather simple model provides an explanation concerning the control of RHO-1 action by spatially and temporally separated RhoGAP activities.

In addition to the function of RGA-3/4 at the anterior cortex in the zygote, we found a requirement for RGA-3/4 in gonad development. Expression of GFP::RGA-3 led to over-proliferation of the gonad and to gonad migration defects. More importantly, whereas neither *rga-3/4(RNAi)* nor *let-502(sb106)* alone, or *cyk-4(RNAi) let-502(sb106)* showed severe gonad defects, *rga-3/4(RNAi) let-502(sb106)* worms contained non-functional and abnormal gonads, similar to those observed in *let-502*$^{-/-}$ animals. RGA-3/4 could either act in the same pathway or in a parallel pathway as LET-502 in the gonad. The manner in which RGA-3/4 and CYK-4 control RHO-1 activity in the early embryo and in the gonad might be different. Further components of these signalling pathways must be identified to shed light on the precise function of the RhoGAPs RGA-3/4 and CYK-4.

We thank G. Seydoux, F. Motegi, P. Mains and the *Caenorhabditis* Genetics Center for *C. elegans* strains. We are grateful to M. Labouesse, T. Sandmann, D. Poteryaev and I. G. Macara for critical reading of the manuscript. We are indebted to R. Ciosk for help with the identification of the gonad phenotypes. This work was supported by the Max Planck Society (Germany) and the Biozentrum of the University of Basel (Switzerland).

Note added in proof

Stephanie Schonegg et al. have obtained similar results to those reported here (Schonegg et al., 2007).

Supplementary material

Supplementary material for this article is available at http://dev.biologists.org/cgi/content/full/134/19/3495/DC1

References

Bernards, A. (2003). GAPs galore! A survey of putative Ras superfamily GTPase activating proteins in man and Drosophila. *Biochim. Biophys. Acta* **1603**, 47-82.
Brenner, S. (1974). The genetics of Caenorhabditis elegans. *Genetics* **77**, 71-94.
Cheeks, R. J., Canman, J. C., Gabriel, W. N., Meyer, N., Strome, S. and Goldstein, B. (2004). C. elegans PAR proteins function by mobilizing and stabilizing asymmetrically localized protein complexes. *Curr. Biol.* **14**, 851-862.
Cowan, C. R. and Hyman, A. A. (2004a). Asymmetric cell division in C. elegans: cortical polarity and spindle positioning. *Annu. Rev. Cell Dev. Biol.* **20**, 427-453.
Cowan, C. R. and Hyman, A. A. (2004b). Centrosomes direct cell polarity independently of microtubule assembly in C. elegans embryos. *Nature* **431**, 92-96.
Cuenca, A. A., Schetter, A., Aceto, D., Kemphues, K. and Seydoux, G. (2003). Polarization of the C. elegans zygote proceeds via distinct establishment and maintenance phases. *Development* **130**, 1255-1265.
Etienne-Manneville, S. and Hall, A. (2002). Rho GTPases in cell biology. *Nature* **420**, 629-635.
Glotzer, M. (2005). The molecular requirements for cytokinesis. *Science* **307**, 1735-1739.
Gönczy, P., Grill, S., Stelzer, E. H., Kirkham, M. and Hyman, A. A. (2001). Spindle positioning during the asymmetric first cell division of Caenorhabditis elegans embryos. *Novartis Found. Symp.* **237**, 164-175; discussion 176-181.
Gotta, M., Abraham, M. C. and Ahringer, J. (2001). CDC-42 controls early cell polarity and spindle orientation in C. elegans. *Curr. Biol.* **11**, 482-488.
Guo, S. and Kemphues, K. J. (1996). A non-muscle myosin required for embryonic polarity in Caenorhabditis elegans. *Nature* **382**, 455-458.
Hung, T. J. and Kemphues, K. J. (1999). PAR-6 is a conserved PDZ domain-containing protein that colocalizes with PAR-3 in Caenorhabditis elegans embryos. *Development* **126**, 127-135.
Jaffe, A. B. and Hall, A. (2005). Rho GTPases: biochemistry and biology. *Annu. Rev. Cell Dev. Biol.* **21**, 247-269.
Jantsch-Plunger, V., Gonczy, P., Romano, A., Schnabel, H., Hamill, D., Schnabel, R., Hyman, A. A. and Glotzer, M. (2000). CYK-4: a Rho family gtpase activating protein (GAP) required for central spindle formation and cytokinesis. *J. Cell Biol.* **149**, 1391-1404.
Jenkins, N., Saam, J. R. and Mango, S. E. (2006). CYK-4/GAP provides a localized cue to initiate anteroposterior polarity upon fertilization. *Science* **313**, 1298-1301.
Jenna, S., Caruso, M. E., Emadali, A., Nguyen, D. T., Dominguez, M., Li, S., Roy, R., Reboul, J., Vidal, M., Tzimas, G. N. et al. (2005). Regulation of membrane trafficking by a novel Cdc42-related protein in Caenorhabditis elegans epithelial cells. *Mol. Biol. Cell* **16**, 1629-1639.
Kamath, R. S., Fraser, A. G., Dong, Y., Poulin, G., Durbin, R., Gotta, M., Kanapin, A., Le Bot, N., Moreno, S., Sohrmann, M. et al. (2003). Systematic functional analysis of the Caenorhabditis elegans genome using RNAi. *Nature* **421**, 231-237.
Kay, A. J. and Hunter, C. P. (2001). CDC-42 regulates PAR protein localization and function to control cellular and embryonic polarity in C. elegans. *Curr. Biol.* **11**, 474-481.
Kemphues, K. (2000). PARsing embryonic polarity. *Cell* **101**, 345-348.
Krugmann, S., Anderson, K. E., Ridley, S. H., Risso, N., McGregor, A., Coadwell, J., Davidson, K., Eguinoa, A., Ellson, C. D., Lipp, P. et al. (2002). Identification of ARAP3, a novel PI3K effector regulating both Arf and Rho GTPases, by selective capture on phosphoinositide affinity matrices. *Mol. Cell* **9**, 95-108.
Miura, K., Jacques, K. M., Stauffer, S., Kubosaki, A., Zhu, K., Hirsch, D. S., Resau, J., Zheng, Y. and Randazzo, P. A. (2002). ARAP1: a point of convergence for Arf and Rho signaling. *Mol. Cell* **9**, 109-119.
Moon, S. Y. and Zheng, Y. (2003). Rho GTPase-activating proteins in cell regulation. *Trends Cell Biol.* **13**, 13-22.
Motegi, F. and Sugimoto, A. (2006). Sequential functioning of the ECT-2 RhoGEF, RHO-1 and CDC-42 establishes cell polarity in Caenorhabditis elegans embryos. *Nat. Cell Biol.* **8**, 978-985.
Munro, E., Nance, J. and Priess, J. R. (2004). Cortical flows powered by asymmetrical contraction transport PAR proteins to establish and maintain anterior-posterior polarity in the early C. elegans embryo. *Dev. Cell* **7**, 413-424.
Narumiya, S. and Yasuda, S. (2006). Rho GTPases in animal cell mitosis. *Curr. Opin. Cell Biol.* **18**, 199-205.
Piekny, A. J. and Mains, P. E. (2002). Rho-binding kinase (LET-502) and myosin phosphatase (MEL-11) regulate cytokinesis in the early Caenorhabditis elegans embryo. *J. Cell Sci.* **115**, 2271-2282.
Piekny, A. J., Wissmann, A. and Mains, P. E. (2000). Embryonic morphogenesis in *Caenorhabditis elegans* integrates the activity of LET-502 Rho-binding kinase, MEL-11 myosin phosphatase, DAF-2 insulin receptor and FEM-2 PP2c phosphatase. *Genetics* **156**, 1671-1689.
Praitis, V., Casey, E., Collar, D. and Austin, J. (2001). Creation of low-copy integrated transgenic lines in Caenorhabditis elegans. *Genetics* **157**, 1217-1226.
Raftopoulou, M. and Hall, A. (2004). Cell migration: Rho GTPases lead the way. *Dev. Biol.* **265**, 23-32.
Schmidt, A. and Hall, A. (2002). Guanine nucleotide exchange factors for Rho GTPases: turning on the switch. *Genes Dev.* **16**, 1587-1609.
Schneider, S. Q. and Bowerman, B. (2003). Cell polarity and the cytoskeleton in the Caenorhabditis elegans zygote. *Annu. Rev. Genet.* **37**, 221-249.
Schonegg, S. and Hyman, A. A. (2006). CDC-42 and RHO-1 coordinate acto-myosin contractility and PAR protein localization during polarity establishment in C. elegans embryos. *Development* **133**, 3507-3516.
Schonegg, S., Constantinescu, A. T., Hoege, C. and Hyman, A. A. (2007). The Rho GTPase activating proteins RGA-3 and RGA-4 are required to set the initial size of PAR domains in *C. elegans* one-cell embryos. *Proc. Natl. Acad. Sci. USA.* In press.
Schwarz, E. M., Antoshechkin, I., Bastiani, C., Bieri, T., Blasiar, D., Canaran, P., Chan, J., Chen, N., Chen, W. J., Davis, P. et al. (2006). WormBase: better software, richer content. *Nucleic Acids Res.* **34**, D475-D478.
Simmer, F., Moorman, C., van der Linden, A. M., Kuijk, E., van den Berghe, P. V., Kamath, R. S., Fraser, A. G., Ahringer, J. and Plasterk, R. H. (2003).

Genome-wide RNAi of C. elegans using the hypersensitive rrf-3 strain reveals novel gene functions. *PLoS Biol.* **1**, E12.

Sonnichsen, B., Koski, L. B., Walsh, A., Marschall, P., Neumann, B., Brehm, M., Alleaume, A. M., Artelt, J., Bettencourt, P., Cassin, E. et al. (2005). Full-genome RNAi profiling of early embryogenesis in Caenorhabditis elegans. *Nature* **434**, 462-469.

Strome, S., Powers, J., Dunn, M., Reese, K., Malone, C. J., White, J., Seydoux, G. and Saxton, W. (2001). Spindle dynamics and the role of gamma-tubulin in early Caenorhabditis elegans embryos. *Mol. Biol. Cell* **12**, 1751-1764.

Timmons, L., Court, D. L. and Fire, A. (2001). Ingestion of bacterially expressed dsRNAs can produce specific and potent genetic interference in Caenorhabditis elegans. *Gene* **263**, 103-112.

Wallenfang, M. R. and Seydoux, G. (2000). Polarization of the anterior-posterior axis of C. elegans is a microtubule-directed process. *Nature* **408**, 89-92.